Available online at www.sciencedirect.com
ScienceDirect
Postharvest Biology and Technology 45 (2007) 381–384
Postharvest Biology and Technology
www.elsevier.com/locate/postharvbio

# Dual energy X-ray image analysis for classifying vitreousness in durum wheat

S. Neethirajan[a], D.S. Jayas[a,*], C. Karunakaran[b]

[a] *The Canadian Wheat Board Centre for Grain Storage Research, Biosystems Engineering, University of Manitoba, Winnipeg, Man., Canada R3T 5V6*

[b] *Canadian Light Source Inc., 101 Perimeter Road, Saskatoon, Sask., Canada S7N 0X4*

Received 4 October 2006; accepted 10 March 2007

**Abstract**

Dual energy X-ray imaging technique is an alternative to simple transmission X-ray imaging. The former has the ability to reveal the internal density changes of a scanned object by exploiting differences in how the scanned material interacts with X-rays at different energies. The feasibility of dual energy X-ray image analysis to classify vitreousness in durum wheat was assessed at 12, 14 and 16% moisture content (m.c.). Algorithms were developed for the logarithmic subtraction of images and for extraction of features. Histogram groups and total gray values were extracted from the dual energy subtracted images. Statistical and neural network classifiers were used for identifying vitreous and non-vitreous kernels from the sample images. Neural network classifiers correctly classified vitreous and non-vitreous kernels with 93% accuracy. The statistical classifiers provided 89% accuracy for vitreous and non-vitreous kernels. The over all classification accuracy for differentiating vitreous and non-vitreous kernels is higher using dual energy X-ray imaging than the simple transmission X-ray imaging.


*Keywords:* Dual energy X-ray images; Vitreous kernels; Non-vitreous kernels; Statistical classifiers; Neural network classifiers

## 1. Introduction

Vitreousness is a key quality parameter used for classifying durum wheat. Vitreous durum wheat kernels are glassy and translucent in appearance while non-vitreous kernels contain a starchy or mottled appearance. There are strict tolerances for the number of non-vitreous kernels allowed into durum grades. Canada imposes 80% or more hard vitreous kernels for Grade 1 Canada Western Amber Durum wheat class for export (CGC, 2005). A quality conscious market requires guaranteeing minimum non-vitreous levels for each shipment. If the grain delivered has more than the specified limit of non-vitreous kernels then the grain may be rejected or price discounted.

Machine vision is one of the most promising technologies to contribute to the accuracy, consistency and objectivity of grain quality inspection. Researchers have used transmitted light images (Symons et al., 2003), transmitted and reflected light images (Xie et al., 2004; Wang et al., 2005) and near infrared spectral images (Dowell, 2000) for classifying vitreousness in durum wheat.

X-ray techniques are gaining momentum and becoming an alternative to other imaging techniques. Because of low radiation and the ability to reveal the internal density changes, soft X-rays are suitable to be used for agricultural product inspection. When an X-ray beam passes through the matter (sample), it undergoes attenuation. Due to attenuation, the intensity of the X-ray energy decreases gradually by absorption and scattering. Absorption refers to the case in which an incident X-ray photon gives up all of its energy. Scattering refers to those X-ray photons that have undergone a change in direction after interaction with atoms of matter. Other photons which are neither absorbed nor scattered, simply pass through the matter and can be detected. This process is known as transmission X-ray imaging (Curry et al., 1990).

The interaction of X-rays with a homogeneous material (Dyson, 1990) can be described as:

$$I(E) = I_0(E)\mathrm{e}^{-\mu(E)x} \tag{1}$$

where $I_0(E)$ is incident beam intensity (mA), $I(E)$ the transmitted beam intensity (mA), $\mu(E)$ the linear attenuation coefficient

* Corresponding author at: 207 Administration Building, University of Manitoba, Winnipeg, Man., Canada R3T 2N2. Tel.: +1 204 474 6860; fax: +1 204 474 7568.

*E-mail address:* digvir_jayas@umanitoba.ca (D.S. Jayas).

0925-5214/$ – see front matter © 2007 Elsevier B.V. All rights reserved.
doi:10.1016/j.postharvbio.2007.03.009

of the material, $x$ the distance traveled by X-rays in the material (mm) and $E$ is the X-ray photon energy (kV). The transmitted X-ray beam intensity decreases with an increase in material thickness or density or both.

A soft X-ray system can detect internal insect infestations (Karunakaran et al., 2004) and can detect sprouted kernels (Neethirajan et al., 2006a), thus provides an opportunity to develop a single system for multiple tasks in the grain industry. In addition, when grain is flowing on a belt under real time conditions, the X-rays can be used to measure grain depth because of differences in the absorption of X-rays. In a recent study, Neethirajan et al. (2006b) have demonstrated that vitreous kernels could be classified using soft X-rays with 82% accuracy at 16% m.c.

An alternative technique to simple transmission X-ray imaging is dual energy X-ray imaging. A small contrast in a X-ray transmitted image can be enhanced by a suitable selection of two X-ray photon energies (Zwiggelaar et al., 1997). Dual energy X-ray imaging has been successfully used to identify calculi in kidneys (Nedavnii and Osipov, 2001), to detect glass contamination in horticultural peat (Ayelaw et al., 2004); to predict carcass composition of pig genetic lines (Marcoux et al., 2005); for measuring soft-tissue composition in small subjects (Koo, 2000); for efficient detection and classification of inclusions in an object with fluctuating parameters (Nedavnii and Osipov, 2005).

The density of the vitreous kernels is higher than the non-vitreous kernels. Non-vitreous kernels are starchy and have broader distribution of densities, while vitreous kernels are hard and have narrower distribution of densities (Dobraszczyk et al., 2002). The hypothesis of this study is that by employing the dual energy X-ray principle, the vitreous kernels can be differentiated from the non-vitreous kernels with higher classification accuracy than simple transmission X-ray imaging.

The objectives of this study are:

(1) to determine the potential of dual energy X-ray images for identifying the vitreous kernels in durum wheat and
(2) to determine the classification percentages of the vitreous and non-vitreous kernels using artificial neural networks and statistical classifiers based on features derived from the subtracted X-ray images.

## 2. Materials and methods

### 2.1. Samples

Durum wheat samples (*Triticum turgidum L.*) collected from Thunder Bay, Canada, conditioned to 12, 14 and 16% moisture content were used in this study. Kernels were manually separated into vitreous and non-vitreous sets based on visual assessment. A total of 1800 kernels (300 in each set) were scanned using a soft X-ray imaging system. X-ray images of wheat kernels were acquired using a Lixi fluoroscope that has 62.5 μm resolution detection screen (Model: LX-85708, Lixi Inc., Downers Grove, IL). Preliminary experiments were done to select the higher and lower X-ray energy levels to enhance the image contrast between vitreous and non-vitreous kernels. The spatial resolution of the images was considered in selecting the settings for high and low-energy X-rays. The two settings used for high and low-energy X-rays were: 13.5 kV, 185 μA and 26 kV, 11 μA. The wheat kernels were placed manually, crease down, on saran wrap on the sample platform and individual kernels were X-rayed at both energies. A total of 3600 images were obtained. The scanned X-ray images of wheat kernels were digitized into 8-bit gray scale images at a resolution of 60 pixels/mm.

### 2.2. Image analysis and feature extraction

Image subtraction is a common image processing method and has been used in many areas of machine vision to enhance small changes between equivalent pairs of images (Lehmann et al., 1997; Bromiley et al., 2002).

We developed algorithms in MATLAB (Version 7.1, The Mathworks Inc., Natick, MA) to subtract the images of the same kernels scanned at high and low-energy levels. To create a dual energy image, weighted subtraction of the logarithm of the low-energy image from that of the high-energy image was performed. Image subtraction was applied on both the vitreous and non-vitreous images.

The subtracted dual energy images were used for feature extraction using the image processing algorithm developed for this study. The normalized histograms were obtained for each kernel image and were grouped into 50 bins (Karunakaran et al., 2004). The other features extracted were: kernel area (Σ pixels), total gray value (Σ gray values in kernel), mean gray value (Σ gray values/Σ pixels), inverted gray value (standard white to black mapping), and standard deviation of the gray levels. A total of 55 image features were extracted from both vitreous and non-vitreous kernels at all moisture contents and used for classification.

### 2.3. Classification

The dual energy X-ray images were grouped into vitreous and non-vitreous sets for classification purposes. The extracted 55 image features were reduced to 17 features using STEPDISC function (SAS, 2000). The Wilk's lambda (0.25) and associated average-squared canonical correlation were used as the criteria of significance. The linear discriminant classifier using parametric method was used with the DISCRIM procedure (SAS, 2000). The discriminant analysis was used to determine the classification accuracy for the two sets. Classification accuracy is the percentage of kernels correctly identified as belonging to a specific class. Classification accuracies were determined by randomly selecting the training and testing sets three times. Three-fourth of the sample was used as training sets and the remaining one-fourth as the independent test sets and the average of the three trials was calculated as the mean classification accuracy.

Jayas et al. (2000) have indicated that four-layer back propagation neural network (BPNN) suits the best for the grain classification applications. The classification accuracies were also determined using a four-layer BPNN. Neural network software package (Neuroshell 2, Version 4.0, Ward Systems Group, Frederick, MD) was used for this purpose. Five random data sets were created by changing the random seed values from zero to five of the data extraction module of Neuroshell 2 software. The data set was grouped and a ratio of 60, 20 and 20% among training, test and validation sets was maintained. A four-layer neural network model with default number of neurons in two hidden layers was used in this study. The network training was done on the training set and the test set was used for testing the trained network. The validation set which was neither used in training nor testing, was used for estimating the classification accuracies. Training was stopped after 1000 epochs. Average classification of five trials was calculated. The results of this classification were compared with the statistical classifier.

## 3. Results and discussions

Fig. 1 shows the subtracted dual energy images of vitreous and non-vitreous kernels. Quantitative information in the dual energy X-ray image does not depend on the image display parameters. Therefore, there is no visually significant difference between the subtracted vitreous and non-vitreous images. However, the histograms of the dual energy subtracted images show that the vitreous kernels have higher gray values than the non-vitreous kernels (Fig. 2)(a and b).

Total inverted gray value and the total area of the kernel images were the two most significant features from STEPDISC procedure. The means of the total gray values and the inverted gray values of the vitreous kernel class were significantly higher than the non-vitreous kernel class. Because of the non-uniform distribution of starch–protein matrix inside the non-vitreous kernels, the rate of absorption of X-rays may be less than that of the vitreous kernels.

The mean area of the vitreous kernel images was 67,241 ± 3967 pixels while the mean area of the non-vitreous kernel images was 57,215 ± 5251 at 12% moisture content. This indicates that the non-vitreous kernels are smaller in area than the vitreous kernels. The same trend was observed for both 14 and 16% m.c. samples. Two different energy levels were applied to take the X-ray image of the same kernel. One energy level may be absorbed more by the soft component (starch) and the other by the hard component (protein). The image features extracted from the subtracted images of vitreous and non-vitreous kernels have the quantification data of the photon energy absorbed in the form of gray levels. The histogram values (90–140 gray value range (Fig. 2(a)) and total gray values, were greater for the vitreous class than for the non-vitreous class. The classification accuracies determined using 17 features by the linear-function

(a) (b)

Fig. 1. Logarithmic subtracted dual energy X-ray images of (a) vitreous and (b) non-vitreous kernels.

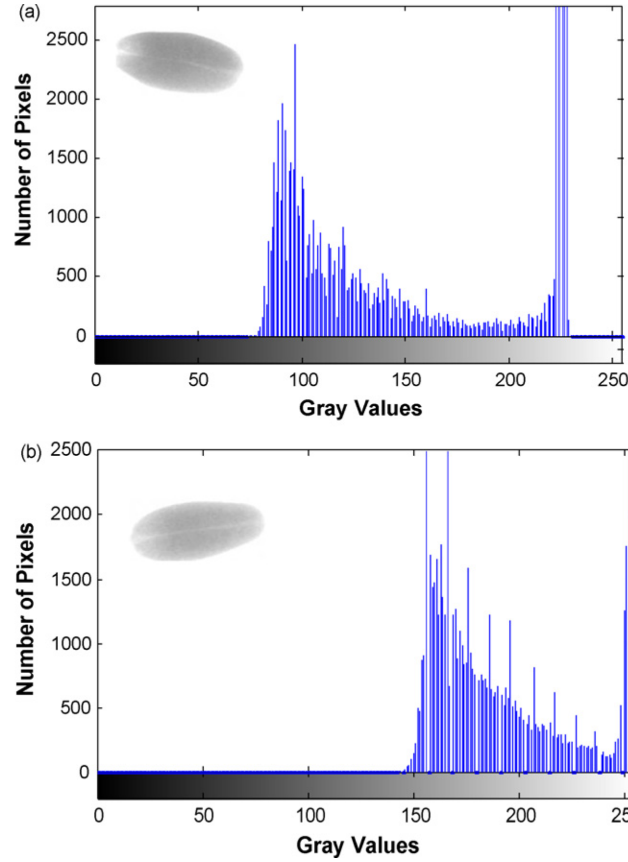


Fig. 2. Inverted gray values of vitreous (a) and non-vitreous (b) durum wheat kernels at 12% moisture content.

parametric statistical classifier and the BPNN are also shown in Table 1. Classification accuracies are higher using the BPNN than the statistical classifier except for 14 and 16% m.c. vitreous and 12% m.c. non-vitreous kernels. The linear-function parametric classifier correctly identified 89% of vitreous and non-vitreous kernels at all moisture contents except 16% m.c. vitreous where classification accuracy was 92%. The BPNN classifier correctly identified 93% of the vitreous kernels and non-vitreous kernels at all moisture content levels. The moisture content had no significant effect ($p > 0.05$) on the classification accuracy of both the vitreous and non-vitreous kernels. The clas-

Table 1
Comparison of classification percentages of vitreous kernels in durum wheat using statistical and BPNN classifiers

| Type | Moisture content (%) | Linear discriminant and parametric (PAR)* | Back propagation neural network (BPNN)* |
|---|---|---|---|
| Vitreous | 12 | $89 \pm 1.2^{a,u}$ | $93 \pm 2.3^{a,v}$ |
| | 14 | $90 \pm 1^{a,u}$ | $91 \pm 1.5^{a,u}$ |
| | 16 | $92 \pm 1.5^{b,u}$ | $94 \pm 2.4^{a,u}$ |
| | 12 | $90 \pm 2.4^{a,u}$ | $94 \pm 1.5^{a,u}$ |
| Non-vitreous | 14 | $88 \pm 3^{a,u}$ | $93 \pm 1^{a,v}$ |
| | 16 | $89 \pm 2.3^{a,u}$ | $94 \pm 1.5^{a,v}$ |

* Numbers followed the same superscript characters (a and b) in each column and (u and v) in each row are statistically similar ($\alpha = 0.05$).

sification accuracies of vitreous and non-vitreous kernels at 16% m.c. using single energy scan (13.5 and 26 kV setting) by statistical classifier were only 75 and 82%, respectively (Neethirajan et al., 2006b). This study proves our hypothesis that dual energy X-ray imaging improves the classification accuracy over single energy transmission X-ray imaging.

## 4. Conclusions

Neural network classifiers correctly classified vitreous and non-vitreous kernels with 93% accuracy. The statistical classifiers provided 89% accuracy for vitreous and non-vitreous kernels. The overall classification accuracy for differentiating vitreous and non-vitreous kernels is higher using dual energy X-ray imaging than the simple transmission X-ray imaging. This study shows that dual energy X-ray images have a great potential for classifying vitreous kernels in durum wheat.

## Acknowledgements

The authors thank the Canada Research Chairs Program and the Natural Sciences and Engineering Research Council of Canada for their financial support for this study. The authors also thank the Industry Services Division of the Canadian Grain Commission for providing durum wheat samples. We thank Kelly Griffiths for helping in sample preparation and data collection.

## References

Ayelaw, G., Holden, N.M., Grace, P., Ward, S.M., 2004. Detection of glass contamination in horticultural peat with dual-energy X-ray absorptiometry (DXA). Comp. Elec. Agric. 42, 1–17.

Bromiley, P.A., Thacker, N.A., Courtney, P., 2002. Non-parametric image subtraction using gray level scattergrams. Image. Vis. Comp. 20, 609–617.

CGC 2005. Official Grain Grading Guide. ISSN 1704-5118.

Curry, T.S., Dowdey, J.E., Murry, R.C., 1990. Christensen's Physics of Diagnostic Radiology. Lea and Febiger, Malvern, PA.

Dobraszczyk, B.J., Whitworth, M.B., Vincent, J.F.V., Khan, A.A., 2002. Single kernel wheat hardness and fracture properties in relation to density and the modelling of fracture in wheat endosperm. J. Cereal. Sci. 35, 245–263.

Dowell, F.E., 2000. Differentiating vitreous and nonvitreous durum wheat Kernels by using near infrared spectroscopy. Cereal. Chem. 77, 155–158.

Dyson, N.A., 1990. X-rays in Atomic and Nuclear Physics. Cambridge University Press, Cambridge, UK.

Jayas, D.S., Paliwal, J., Visen, N.S., 2000. Multi-layer neural networks for image analysis of agricultural products. J. Agric. Eng. Res. 7, 119–128.

Karunakaran, C., Jayas, D.S., White, N.D.G., 2004. Identification of wheat kernels damaged by the red flour beetle using X-ray images. Biosyst. Eng. 87, 267–274.

Koo, W.W.K., 2000. Body composition measurements during infancy. Ann. N.Y. Acad. Sci. 904, 383–392.

Lehmann, T., Sovakar, A., Schmiti, W., Repges, R., 1997. A comparison of similarity measures for digital subtraction radiography. Comput. Biol. Med. 27, 151–167.

Marcoux, M., Faucitano, L., Pomar, C., 2005. The accuracy of predicting carcass composition of three different pig genetic lines by dual-energy X-ray absorptiometry. Meat Sci. 70, 655–663.

Nedavnii, O.I., Osipov, S.P., 2005. Use of the two energy X-ray method for detection and classification of inclusions in an inspected object with fluctuating parameters. Russ. J. Nondes. Test 41, 76–83.

Nedavnii, O.I., Osipov, S.P., 2001. Algorithm for identification of calculi in kidneys by the method of digital two-frequency X-ray imaging. Russ. J. Nondes. Test 37, 366–371.

Neethirajan, S., Jayas, D.S., White, N.D.G., 2007. Detection of sprouted wheat kernels using soft X-ray image analysis. J. Food. Eng. 81, 509–513.

Neethirajan, S., Karunakaran, C., Symons, S., Jayas, D.S., 2006b. Classification of vitreousness in durum wheat using soft X-rays and transmitted light images. Comp. Elec. Agric. 53, 71–78.

SAS, 2000. SAS User's Guide: Statistics. SAS Institute Inc., Cary, North Carolina.

Symons, S.J., Van Schepdael, L., Dexter, J.E., 2003. Measurement of hard vitreous kernels in durum wheat by machine vision. Cereal. Chem. 80, 511–517.

Wang, N., Zhang, F., Dowell, F.E., Pearson, T., 2005. Determining vitreousness of durum wheat using transmitted and reflected light images. Trans. ASABE 48, 219–222.

Xie, F., Pearson, T., Dowell, F.E., Zhang, N., 2004. Detecting vitreous kernels using reflectance and transmittance image analysis. Cereal. Chem. 81, 594–597.

Zwiggelaar, R., Bull, C.R., Mooney, M.J., Czarnes, S., 1997. The detection of soft materials by selective energy X-ray transmission imaging. J. Agric. Eng. Res. 66, 203–212.